

Competition between phase-matching and stationarity in Kerr-driven optical pulse filamentation

Daniele Faccio,^{1,*} Alessandro Averchi,¹ Arnaud Couairon,² Audrius Dubietis,³ Rimtautas Piskarskas,³ Aidas Matijosius,³ Francesca Bragheri,⁴ Miguel A. Porras,⁵ Algis Piskarskas,³ and Paolo Di Trapani^{3,†}

¹CNISM and Department of Physics and Mathematics, University of Insubria, Via Valleggio 11, 22100 Como, Italy

²Centre de Physique Théorique, CNRS UMR 7644, École Polytechnique, F-91128, Palaiseau, France

³Department of Quantum Electronics, Vilnius University, Sauletekio Avenue 9, building 3, LT-10222, Vilnius, Lithuania

⁴Department of Electronics, University of Pavia, Via Ferrata 1, 27100 Pavia, Italy

⁵Departamento de Física Aplicada, ETSIM, Universidad Politécnica de Madrid, Ríos Rosas 21, 28003 Madrid, Spain

(Received 26 July 2006; published 25 October 2006)

Experiments show that the spatiotemporal spectral broadening of an intense pump pulse in a Kerr medium in the presence of strong higher-order dispersion does not lead to symmetric profiles, and hence cannot be interpreted as standard modulational instability of a plane and monochromatic nonlinear eigenmode. The highly asymmetric features of the generated (K_{\perp}, Ω) spectrum are due to odd-order dispersion terms and are interpreted in terms of spontaneous formation of stationary conical waves.

DOI: [10.1103/PhysRevE.74.047603](https://doi.org/10.1103/PhysRevE.74.047603)

PACS number(s): 42.65.Tg, 05.45.Yv, 41.20.Jb

The spectral broadening accompanying the nonlinear dynamics of intense optical wave packets in bulk Kerr media is often described in terms of the modulational instability (MI) of the plane and monochromatic (PM) nonlinear eigenmode [1]. For the most frequently encountered case of focusing nonlinear response, the PM MI was shown to lead to hyperbolic or elliptic profiles for the largest-gain (K_{\perp}, Ω) surface for normal and anomalous dispersion, respectively [2]. In the quoted model, the effect of chromatic dispersion was taken into account only up to the second order. When higher-order dispersion is included, calculations show that only even terms contribute to PM MI [3,4].

In real settings, one should expect spectral broadening to be suitably described by PM MI as long as the pump field is close to the PM-wave limit and the nonlinear response is that of an ideal Kerr medium. In most of the recently experimentally investigated regimes, associated with femtosecond pulse filamentation, in contrast, the launched input wave packet is a very short pulse and a focused beam. In these conditions, one might expect odd terms to have a chance of provoking the breaking of the symmetry in the spectral broadening process. Notably, asymmetry is evident in recent numerical and experimental investigations concerning ultrashort-pulse dynamics in water [5–7].

The PM MI failure at describing the largest-amplified surface (e.g., the correct curvature) in the (K_{\perp}, Ω) region close to the pump has been in fact reported in [8], where a double-hyperbolic frequency-gap structure is observed rather than a single K_{\perp} -gap hyperbola. The departure of the PM MI prediction from the observations was attributed to the strong localization of the pump. Here our measurements outline a marked asymmetry between redshifted and blueshifted portions of the generated spectrum. Notably, owing to their very broad spectrum, these waves share the characteristics of X waves in the normal dispersion regime and O waves in the

anomalous dispersion regime [9], as also seen in the broadband linear modes proposed by Orlov *et al.* [11].

The experiments were performed in two different nonlinear Kerr media, i.e., in pure water and fused silica. The input laser pulse was delivered from a Nd:glass laser (Twinkle; Light Conversion Ltd.) and a tunable optical parametric generator (TOPAS; Light Conversion Ltd.). The pulse had 200 fs duration [full width at half maximum (FWHM)] and was loosely focused down to 100 μm diameter (FWHM) at the sample input facet. In order to induce filamentation the input energy E_{in} was typically varied from 2 to 20 μJ so that the input power was $P \sim (5-20)P_{crit}$ with $P_{crit} = 3.77\lambda_0^2/8\pi n_0 n_2$, where n_0 and n_2 denote the linear and nonlinear refractive indices, respectively. λ_0 is the incident laser wavelength and was chosen as 1055 nm for water, i.e., just slightly larger than the zero-dispersion wavelength (~ 1000 nm) [12], and as 1600 nm for fused silica, i.e., well within the anomalous dispersion regime. In the water experiment, owing to negligible second-order dispersion, we expect third-order or more generically high-order dispersion (HOD) to play a dominant role, thus making the regime ideal for demonstrating the failure of PM-MI-based predictions. In the fused-silica experiment, in contrast, the wavelength was chosen far from the zero-dispersion region (located at ~ 1290 nm [13]). Even in this case, however, the nonlinear dynamics provided evidence of a relevant HOD effect. The filament generated inside the Kerr medium was collected from the output sample facet and imaged by a double-lens telescope onto the focal plane of an $f=15$ cm focal-length lens. This lens was in turn positioned at a distance f from the input slit of an imaging spectrometer (Lot-Oriel, model MS260i). At the output of the spectrometer we recorded on a charge-coupled device (CCD) camera the (θ, λ) far-field profile, or angular spectrum (AS), which can be easily mapped into the (K_{\perp}, Ω) spectrum [14]. In Fig. 1(a) we show a single-shot AS of a filament generated in 4 cm of water, for the case of $E_{in}=15$ μJ . The AS is highly asymmetric, with ringlike interference fringes surrounding the pump, and a hyperbolic-like tail peaked at ~ 850 nm and extending further in the blueshifted region. The input-pump AS is shown in the

*Electronic address: daniele.faccio@uninsubria.it

†Permanent address: Department of Physics & Mathematics, University of Insubria, Via Valleggio 11, 22100 Como, Italy.

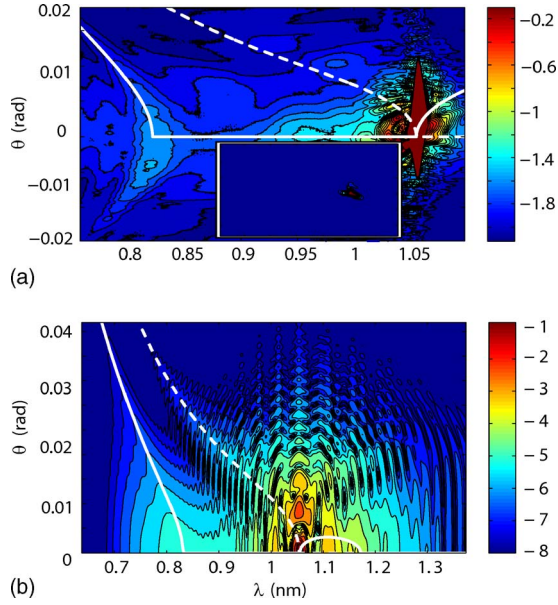


FIG. 1. (Color online) (a) Experimentally measured log-scale spectrum of a filament in 4 cm of water, with an input pump centered at $1.055 \mu\text{m}$ and with $E_{in}=15 \mu\text{J}$. The inset shows the input spectrum on the same scale, but with shifted axis. (b) Same as in (a) but calculated numerically from Eq. (1). White solid lines indicate the stationary fish mode, as described in the text.

inset to Fig. 1(a) for comparison. We note the strong resemblance to numerically calculated spectra under similar input conditions [7]. In Fig. 2 we show a similar spectrum for the case of fused silica with $E_{in}=5 \mu\text{J}$. The spectrum was here frequency doubled before the spectrometer using a $20\text{-}\mu\text{m}$ -thick Beta-Barium Borate (BBO) crystal, so as to shift AS wavelengths into the silicon-based CCD sensitivity range. In order to capture the exceptionally large spectral bandwidth, Fig. 2 is composed of spectral samples belonging to different shots, but all with very similar ($\pm 3\%$) input energies. As in Fig. 1 we note the marked asymmetry, with elliptical features around the input wavelength and a hyperbolic modulation at blueshifted wavelengths.

In order to gain a deeper insight into the nonlinear dynamics we performed numerical simulations by solving the nonlinear equation for the Fourier-transformed envelope $\hat{\mathcal{E}}(r, \omega, z) \equiv \mathcal{F}[\mathcal{E}(r, t, z)]$, where details are given in Ref. [5]:

$$2i\hat{U}\partial\hat{\mathcal{E}}/\partial z + [\nabla_{\perp}^2 + (k^2 - \hat{U}^2)]\hat{\mathcal{E}} = -\mathcal{F}\{N(\mathcal{E})\}, \quad (1)$$

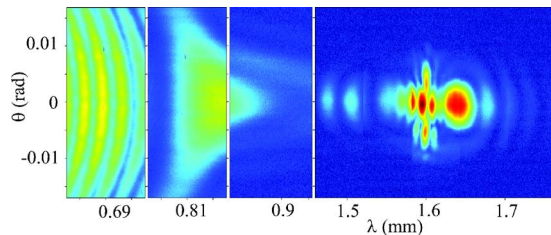


FIG. 2. (Color online) Experimentally measured spectrum of a filament in 3 cm of fused silica with an input pump centered at $1.6 \mu\text{m}$ and with $E_{in}=5 \mu\text{J}$.

$$N(\mathcal{E}) = k_0 \left(2 \frac{k_0 n_2}{n_0} T^2 |\mathcal{E}|^2 - \frac{k_0 \rho}{n_0^2 \rho_c} + iT\beta_K |\mathcal{E}|^{2K-2} \right) \mathcal{E}. \quad (2)$$

The model accounts for diffraction, dispersion via the relation $k(\omega) \equiv n(\omega)\omega/c$, Kerr self-focusing ($n_2 = 3.2 \times 10^{-16} \text{ cm}^2/\text{W}$), multiphoton absorption ($\beta_K = 2 \times 10^{-60} \text{ cm}^{19}/\text{W}^{10}$, $K=10$), defocusing by the plasma with density ρ described by $\partial\rho/\partial t = (\beta_K/K\hbar\omega_0)|\mathcal{E}|^{2K}$, and space-time focusing and self-steepening via the operators $\hat{U} \equiv k_0 + k'_0(\omega - \omega_0)$ and $T \equiv 1 + (i/\omega_0)\partial/\partial t$. $\rho_c \equiv (\epsilon_0 m/e^2)\omega_0^2$ denotes the wavelength-dependent critical plasma density. Figure 1(b) displays the results of a numerical simulation with parameters corresponding to the experiment shown in Fig. 1(a). Only marginal differences in the final spectrum were obtained by switching on or off the effect of plasma defocusing in Eq. (1). As can be seen, the main features of the measured AS are well reproduced by our model, with optimum agreement regarding the location and shape of the blueshifted tail. Furthermore, the simulation showed that during filamentation the input pulse splits into two main peaks propagating with different group velocities, whose overlapping spectra create the ringlike interference fringes clearly visible around the pump.

We have recently introduced an interpretation of these experimental and numerical results based on the assumption that the laser pulse evolution is characterized by the spontaneous formation of stationary conical waves.

It is furthermore possible to interpret the pulse splitting in normal dispersion in terms of phase-matched parametric interaction among an intense pump and two linear, signal and idler, X waves [8]. In the quadratic-dispersion approximation, the two waves split with opposite velocity in the reference frame of the input pump, leading to a symmetric spectrum. Here we generalize that approach to the case where HOD plays a relevant role. To this end we introduce the transverse dispersion relation for linear stationary modes [10]

$$K_{\perp} = \sqrt{k^2(\Omega) - k_z^2(\Omega)} \quad (3)$$

where $\Omega = \omega - \omega_0$ is the frequency shift with respect to the carrier frequency, $k(\Omega) = (\omega/c)n(\omega)$, and the longitudinal wave number must be a linear function of detuning Ω for stationarity, which is conveniently written in the form $k_z(\Omega) = (k_0 - \beta) + (k'_0 - \alpha)\Omega$. The parameter β determines the longitudinal wave number $k_0 - \beta$ at ω_0 and α determines the group velocity $1/(k'_0 - \alpha)$ of the wave mode. For the case of water $n(\omega)$ has been taken from an analytical relation obtained by fitting measurements from a white light interferometry setup [12]. For fused silica, $n(\omega)$ has been evaluated using the related Sellmeier relation [13]. The numerical simulations (not shown but similar to those shown in Ref. [7]) highlight a clear temporal splitting of the input pulse into two daughter waves, each of them characterized by a distinct group velocity. In analogy to Ref. [8] we estimated the group velocity of the split pulses from the simulations, and assuming the signal and idler waves to travel locked with each split pump pulse we obtained two values α_s and α_i . According to [8] we also set $\beta_s = 0$, $\beta_i = 0$. The resulting dis-

persion curves $K_{\perp s}$ and $K_{\perp i}$ are shown for the case of water in Fig. 1(a), where the full line corresponds to the wave mode locked with the trailing pulse ($\alpha=-1$ ps/m), the dashed line to the leading one ($\alpha=5$ ps/m). The characteristic “fishlike” structure of the measured and computed AS, made by an (elliptical) redshifted head and a (hyperbolic) blueshifted tail, is suitably reproduced by the stationary modes. Notably, both the location and the shape of the tail are precisely reproduced by the analytical relations, which is remarkable due to the absence of any free parameter in the model. Regarding the redshifted elliptical structure of the mode we note that this is covered by an intense fringe pattern and is thus practically invisible. The elliptical structures are more clearly seen in the case of fused silica. Figure 2 clearly demonstrates occurrence of the pulse-splitting event. Here the AS appears to be made by two elliptical structures, tangent at the input-pump wavelength.

We have performed additional numerical simulations to ascertain the mechanism underlying MI symmetry breaking and the formation of fishlike wave modes. As in Ref. [8] for the double-X structure in the spectrum, symmetry breaking is shown here to be directly linked to the tight localization of the pump in space and time. Simulations consisted in launching an intense input pump on top of a white noise (in both time and space) with the aim of observing which (K_{\perp}, Ω) couples experience the highest gain. All parameters were chosen to match the experimental conditions for water. The propagation distance was shortened so that any self-action effects such as self-phase-modulation, pulse splitting, or self-focusing do not occur, i.e., under conditions of a (nearly) stationary pump pulse. In order to highlight the effect of odd-order dispersion terms, only the second and third dispersion were accounted for.

We note that this approach is not in contradiction with other models based for example on a scattering of the input pump wave from a material polarization wave [15]. Here we use a relatively large background noise in order to efficiently probe the maximum gain curves. The weaker scattering process is not prevented by the model so that without background noise, the scattered waves which are found to be within the gain region will be likewise amplified.

Figures 3(a) and 3(b) show the results for an input pulse that has a radius r_{FWHM} of 1 mm and a duration t_{FWHM} of 400 fs, i.e., very large in both time and space, and may be assimilated to a plane and monochromatic wave. After 1.7 cm propagation the pump pulse is practically unchanged but the background noise has grown along symmetric trajectories that, as expected, resemble very closely those predicted by Liou *et al.* [2], i.e., an X shape if the pump central wavelength λ_0 lies in normal dispersion [Fig. 3(a)] and an O shape if λ_0 lies in anomalous dispersion [Fig. 3(b)]. This result may be interpreted by noting that for a plane monochromatic pump momentum and energy conservation are strictly enforced in the four-wave mixing processes that lead to gain at new frequencies [2]. This in turn implies perfect symmetry in the gain profile. Figure 3(c) shows the same simulation with an input pump pulse of much smaller radius $r_{FWHM}=50 \mu\text{m}$ and duration $t_{FWHM}=20$ fs: after 1.7 cm the spectrum now clearly shows a highly asymmetric gain profile that resembles closely the stationary conical wave modes

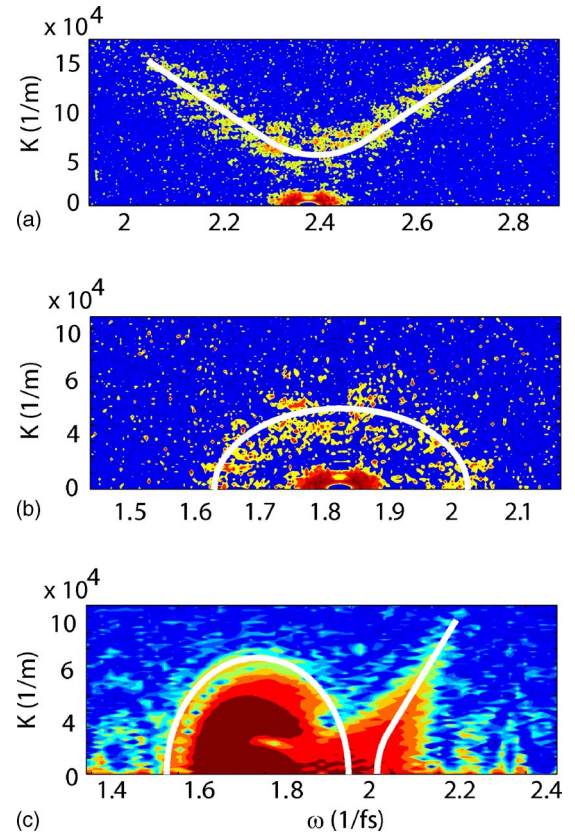


FIG. 3. (Color online) Gain profiles for a background white noise with an input Gaussian pump with (a) $r_{FWHM}=1$ mm, $t_{FWHM}=200$ fs, $\lambda_0=800$ nm, (b) $r_{FWHM}=1$ mm, $t_{FWHM}=200$ fs, $\lambda_0=1055$ nm, and (c) $r_{FWHM}=50 \mu\text{m}$, $t_{FWHM}=20$ fs, $\lambda_0=1055$ nm. Solid lines are a guide for the eye and qualitatively reproduce curves obtainable from Eq. (3).

proposed in Eq. (3). In this case the short pulse duration (i.e., large temporal spectrum) and small radius can be interpreted as leading to a larger indetermination in the energy conservation and in the transverse momentum conservation which may be, to some extent, violated. Therefore, relaxation of the energy and/or of the transverse momentum conservation constraint allows the pulse to spontaneously evolve toward a mode that preserves phase stationarity and that, due to propagation over long distances, will eventually experience the highest gain.

In conclusion, we have shown that spectral broadening of a focused intense ultrashort pulse propagating in a focusing Kerr medium differs substantially from that predictable in terms of the Kerr-driven modulational instability of the plane and monochromatic nonlinear eigenmode or, in other words, of a phase-matched four-wave mixing process. In particular, a marked asymmetry is observed in the angular spectra of filaments generated in both water and fused silica. The dynamics is correctly interpreted in terms of the spontaneous formation of fishlike linear conical waves, i.e., of the broadband linear stationary modes supported by the system. The results outline the key role of the action of third- and higher-order dispersion, whose uneven contribution to phase rotation of the interacting signal (K_{\perp}, Ω) and idler $(-K_{\perp}, -\Omega)$

modes breaks the symmetry that is inherent to energy and momentum conservations in the ideal case of a plane and monochromatic pump and lossless nonlinear response.

The authors gratefully acknowledge financial support from MIUR (Contract No. II 04CFHH9B) and from the

Access to Research Infrastructures activity in the Sixth Framework Program of the EU (Contract No. RII3-CT-2003-506350, Laserlab Europe). P.D.T. is financed by European Union Marie Curie Chair action (STELLA), Contract No. MEXC-2005-025710, <http://europa.eu.int/mariecurie-actions>.

-
- [1] G. G. Luther, A. C. Newell, J. V. Moloney, and E. M. Wright, *Opt. Lett.* **19**, 789 (1994).
- [2] L. W. Liou, X. D. Cao, C. J. McKinstrie, and G. P. Agrawal, *Phys. Rev. A* **46**, 4202 (1992).
- [3] M. J. Potasek, *Opt. Lett.* **12**, 921 (1987).
- [4] S. Wen and D. Fan, *J. Opt. Soc. Am. B* **19**, 1653 (2002).
- [5] A. Couairon, E. Gaizauskas, D. Faccio, A. Dubietis, and P. Di Trapani, *Phys. Rev. E* **73**, 016608 (2006).
- [6] D. Faccio, A. Matijosius, A. Dubietis, R. Piskarskas, A. Varanavicius, E. Gaizauskas, A. Piskarkas, A. Couairon, and P. Di Trapani, *Phys. Rev. E* **72**, 037601 (2005).
- [7] M. Kolesik, E. M. Wright, and J. V. Moloney, *Opt. Express* **13**, 10729 (2005).
- [8] D. Faccio, M. A. Porras, A. Dubietis, F. Bragheri, A. Couairon, and P. Di Trapani, *Phys. Rev. Lett.* **96**, 193901 (2006).
- [9] M. A. Porras and P. Di Trapani, *Phys. Rev. E* **69**, 066606 (2004).
- [10] S. Longhi, *Opt. Lett.* **29**, 147 (2004).
- [11] S. Orlov, A. Piskarskas, and A. Stabinis, *Opt. Lett.* **27**, 2167 (2003).
- [12] A. G. Van Engen, S. A. Diddams, and T. S. Clement, *Appl. Opt.* **37**, 5679 (1998).
- [13] G. P. Agrawal, *Nonlinear Fiber Optics* (Academic Press, New York, 1989).
- [14] D. Faccio, P. Di Trapani, S. Minardi, A. Bramati, F. Bragheri, C. Liberale, V. Degiorgio, A. Dubietis, and A. Matijosius, *J. Opt. Soc. Am. B* **22**, 862 (2005).
- [15] M. Kolesik, E. M. Wright, and J. V. Moloney, *Phys. Rev. Lett.* **92**, 253901 (2004).